Interaction of factor V B-domain acidic region with its basic region and with TFPI/TFPI2: Structural insights from molecular modeling studies

Authors:

Kanagasabai Vadivel,[1] Yogesh Kumar,[1] Matthew W. Bunce,[2] Rodney M. Camire,[2] Madhu S. Bajaj,[3] and S. Paul Bajaj,*[1,4]

Authors note:

[1] UCLA/Orthopaedic Hospital Department of Orthopaedic Surgery, David Geffen School of Medicine, University of California, Los Angeles, CA, USA.

[2] The Center for Cell and Molecular Therapeutics, Division of Hematology, Children's Hospital of Philadelphia and the Department of Pediatrics, University of Pennsylvania, School of Medicine, Philadelphia, PA, USA.

[3] Department of Medicine, Division of Pulmonology and Critical Care, David Geffen School of Medicine, University of California, Los Angeles, CA, USA.

[4] Molecular Biology Institute, University of California, Los Angeles, CA, USA.

Corresponding Author:

S. Paul Bajaj, Department of Orthopaedic Surgery, David Geffen School of Medicine, University of California, Los Angeles, CA 90095. Tel: (310) 825-5622; Fax: (310) 825-5762; Email: pbajaj@mednet.ucla.edu

Authors e-mails:

Kanagasabai Vadivel	E-mail: vksabai@ucla.edu
Yogesh Kumar	E-mail:dr.yogeshkumar@gmail.com
Matthew W. Bunce	E-mail: buncemw@gmail.com
Rodney M. Camire	E-mail: rcamire@mail.med.upenn.edu
Madhu S. Bajaj	E-mail: mbajaj@mednet.ucla.edu
S. Paul Bajaj	E-mail: pbajaj@mednet.ucla.edu

Running Title: FV_{AR2} interaction with FV_{BR}, $TFPI_{BR}$ and $TFPI2_{BR}$

ABSTRACT

Background: Factor V (FV) B-domain contains an acidic region (FV-AR2) and a basic region (FV-BR), which interact with each other and maintain FV in a procofactor form; removal of either region via deletion/proteolysis results in an active FVa molecule. Tissue factor pathway inhibitor type-1 (TFPI) and type-2 (TFPI2) each contain a C-terminus basic segment homologous to FV-BR; this region in TFPI (and predicted in TFPI2) binds to FV-AR2 in platelet FVa (that lacks FV-BR) with high affinity and inhibits FVa function.

Objectives: To understand molecular interactions between FV-AR2 with FV-BR, TFPI-BR and TFPI2-BR.

Methods: Circular dichroism (CD) and molecular modeling approaches.

Results and Conclusions: CD experiments reveal the presence of ~20% helical content in both FV-AR2 and FV-BR but each lacks beta-sheet. Predicted structures of FV-AR2 and FV-BR, obtained using threading (I-TASSER), are consistent with the CD data and have compact folds with hydrophobic residues in the interior and charged residues on the surface. Scores from QMEAN and ModFOLD servers indicate a very high probability for each structure to be native. Predicted models of Kunitz domain-3 of TFPI and TFPI2 each with C-terminal basic tail are consistent with known homologous structures. Docking experiments using ClusPro indicate that the acidic groove of FV-AR2 has high shape complementarity to accommodate the conserved basic residues in FV-BR (1002-RKKKK-1006), TFPI-BR (256-RKRKK-260) or TFPI2-BR (191-KKKKK-195). Further, similar electrostatic interactions occur in each case. These models, in the absence of experimentally determined structures, provide a guiding point for proper mutagenesis studies in FV, TFPI and TFPI2.

Keywords: Blood coagulation, Factor V, molecular models, TFPI, TFPI2

1. Introduction

Full-length tissue factor pathway inhibitor type-1 (TFPI) and type-2 (TFPI2) are structural homologs, each consisting of three Kunitz domains and a very basic C-terminal region[1,2] (Figure 1) that is deemed functionally vital in binding to the B-domain acidic region of factor (F) V.[3,4] The function of the first-domain of TFPI is to inhibit FVIIa/tissue factor, whereas the second-domain inhibits FXa and the third-domain has no inhibitory activity.[1] The function of the first-domain of TFPI2 is to inhibit plasmin, FXIa and kallikrein, while the other two domains have no inhibitory activity.[2] Residues 710-1545 comprise the B-domain of FV and are located between the N-terminus A1-A2 domains (residues 1-709) and the C-terminus A3-C1-C2 domains (residues 1546-2196)[5] (Figure 1). In addition, there is an acidic residue region (FV-AR1, residues 659-664/688-697) located between the A2-domain and the B-domain of FV[5]; precise function of this region is not known. Further, the B-domain has two conserved regions, namely, the basic residue region (FV-BR, residues 963-1008) and a second acidic residue region (FV-AR2, residues 1493-1537), which interact with each other and lock FV in an inactive state; removal of the FV-AR2 (previously termed FV-AR) or the FV-BR region yields constitutively active FVa-like molecule.[6] Importantly, binding of FV-BR peptide to the active FVa-like molecule (FV-810) harboring the FV-AR2 region results in loss of activity and its ability to bind FXa to form the prothrombinase complex.[7] These experimental observations unravel the molecular basis of physiologic activation of FV.

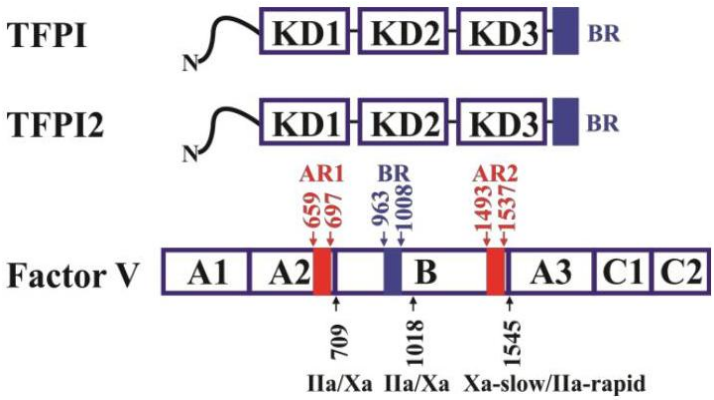

Figure 1**. Schematic representation of the domain organization of TFPI, TFPI2 and factor V**. TFPI and TFPI2 have similar domain organizations and contain three Kunitz domains (KD1, KD2, KD3) and a C-terminal basic region (BR). FV consists of three ceruloplasmin-type domains (A1, A2, A3), a unique B domain and two discoidin-type domains (C1, C2). The acidic regions 1 and 2 (AR1 659-697, AR2 1493-1537) are depicted in red whereas the basic region (BR 963-1008) is depicted in blue. The IIa/Xa proteolytic cleavage sites (Arg709, Arg1018 and Arg1545) are also depicted. IIa, thrombin; Xa, factor Xa.

During blood coagulation, FV is initially cleaved at Arg^{709} and Arg^{1018} by thrombin or FXa[8,9] (Figure 1) to yield constitutively active FVa molecule ($FVa_{des710-1018}$) that lacks the B-domain BR region.[3,6,7] $FVa_{des710-1018}$ is rapidly cleaved at Arg^{1545} by thrombin to yield the final active FVa molecule, which lacks both the FV-AR2 and FV-BR regions.[3,6,7] In contrast, proteolysis at Arg^{1545} by FXa is slow and results in accumulation of $FVa_{des710-1018}$ during the initial phase of coagulation that retains the FV-AR2 region; this is also the major form of FV in platelets.[10]

Nine residues in FV-BR (998-LIKTRKKKK-1006) are highly homologous to the C-terminal basic region (BR) of TFPI

(252-LIKTKRKRK-260) or TFPI2 (187-AKALKKKKK-195).[1-6] Remarkably, similar to FV-BR, TFPI-BR binds to $FVa_{des710-1018}$ and FV-810 that lacks the amino acids 811-1491 including the BR region 963-1008 residues,[7] and inhibits FVa:FXa formation.[3] Further, two naturally occurring variants of FV each containing FV-AR2 (but lacking FV-BR) circulate in blood bound to TFPI[11,12]; such variant FV/TFPI complexes prevent FV function and result in a bleeding diathesis. Furthermore, TFPI (but not $TFPI_{161}$ that lacks Kunitz domain-3 and the BR segment) inhibits binding of TFPI2 to FV[4] implicating the importance of C-terminal basic region in its binding to FV. Thus, it would appear that FV-BR, TFPI-BR and TFPI2-BR employ similar interactions critical in binding to FV-AR2; this also implies that the other region(s) in TFPI and TFPI2 may not play a central role in forming these complexes. Further, purification of TFPI2 from platelet lysates using anhydro-plasmin affinity column yields TFPI2 that is associated with platelet FV.[4] These observations indicate that TFPI2 present in platelets could inhibit FXa:$FVa_{des710-1018}$ formation. Thus, interactions of FV-AR2 with FV-BR and with TFPI or TFPI2 are biologically significant. However, the molecular details of these interactions are not known. Here, we employed circular dichroism (CD) spectroscopy and molecular modeling approaches to decipher the putative interactions between the FV-AR2 with FV-BR, TFPI-BR and TFPI2-BR.

2. Materials and methods

2.1 CD experiments

The FV-AR2 and FV-BR peptides were expressed and purified as described.[7] The CD spectra of FV-BR and FV-AR2 each at a concentration of 0.2 mg/ml (~30 μM) and of FV-AR2+FV-BR mixture (final concentration 0.1 mg/ml each) were recorded at 25 °C from 190 to 250 nm. The spectra were obtained using J-715 spectrophotometer (JASCO) in a 0.1 cm cell with a band width of 1.0 nm, response time of 4 sec, and a scan speed of 20 nm/min. The buffer used was 20 mM sodium phosphate, pH 8.0 and each spectrum represents the average of four scans. The CD spectrum of 20 mM sodium phosphate buffer, pH 8.0 used as a background was subtracted from the protein spectra. The spectra were analyzed using Dichroweb server utilizing the CONTIN program.[13,14]

2.2 Molecular Modeling

Structures of the FV-AR2 and FV-BR region as well as the Kunitz domain-3 with the C-terminal segment (including the BR region) each of TFPI and TFPI2 were modeled using the I-TASSER server.[15] In the absence of sequence homologs for FV-AR2 and FV-BR, the threading approach was employed to build their structures.[15] The quality of the predicted structures was assessed using QMEAN[16] and ModFOLD servers.[17] Since homologous structures for Kunitz domain-3 segment each of TFPI and TFPI2 are available, they were modeled using the homology modeling approach. The PDB structures 1IRH (TFPI Kunitz domain-3 without the C-terminal tail) and 2ODY (51% identity with TFPI2 Kunitz domain-3) were used as templates to build the Kunitz domain-3 of TFPI and TFPI2 along with their C-terminal basic regions.[18-20] The resulting structures were minimized with the backbone constrains using CHARMM[21] and the top model in each case was chosen for the docking experiments.

2.3 Molecular Docking

The interactions between FV-AR2 and FV-BR, between FV-AR2 and TFPI-BR, and between FV-AR2 and TFPI2-BR were modeled using the ClusPro docking server.[22] The FV-AR2 was considered as the receptor while the FV-BR, TFPI-BR and TFPI2-BR were treated as ligand molecules. When performing the docking experiments, the conserved nine-residue segment in each ligand was specified as the favorable binding region. Each docked model was selected based on the balanced score that was dependent on the electrostatic, Van der Walls contacts and

hydrophobic interactions as well as the shape complementarity score. The models were further subjected to energy minimization with CHARMM to relieve steric clashes.[21]

3. Results and Discussion

The far-UV CD spectra data collected for FV-AR2, FV-BR and the equimolar mixture of FV-AR2+FV-BR are shown in Figure 2. The spectra analyzed using DICHROWEB[13] revealed that both FV-AR2 and FV-BR peptides contain helical content of ~21% and ~24%, respectively. The native polyacrylamide gel electrophoresis (PAGE)-gels of FV-AR2, FV-BR and FV-AR2+FV-BR mixture are shown in Figure 2 inset. As expected, the FV-AR2 migrated rapidly towards the anode (lane 1). Since the FV-BR is positively charged, its mobility was retarded towards the anode and it essentially stayed at the top of the gel (lane 2). However, in the FV-AR2+FV-BR mixture, the mobility of FV-BR was slightly increased, whereas that of FV-AR2 was somewhat decreased (lane 3). This could indicate that the FV-AR2+FV-BR mixture initially moves as a complex and rapidly dissociate into individual moieties during electrophoresis. Further, similar to FV-AR2 and FV-BR, the FV-AR2+FV-BR mixture also contained ~20% helical content (Figure 2); thus, no noticeable change in the secondary structure upon complex formation was observed. Noticeably, TFPI-BR binds to FV-AR2[3] and the binding of TFPI2 to FV is inhibited by full length TFPI but not by $TFPI_{1-161}$ lacking the C-terminal BR region.[4] These observations indicate that TFPI-BR and TFPI2-BR would interact similarly as seen for FV-BR to FV-AR2.

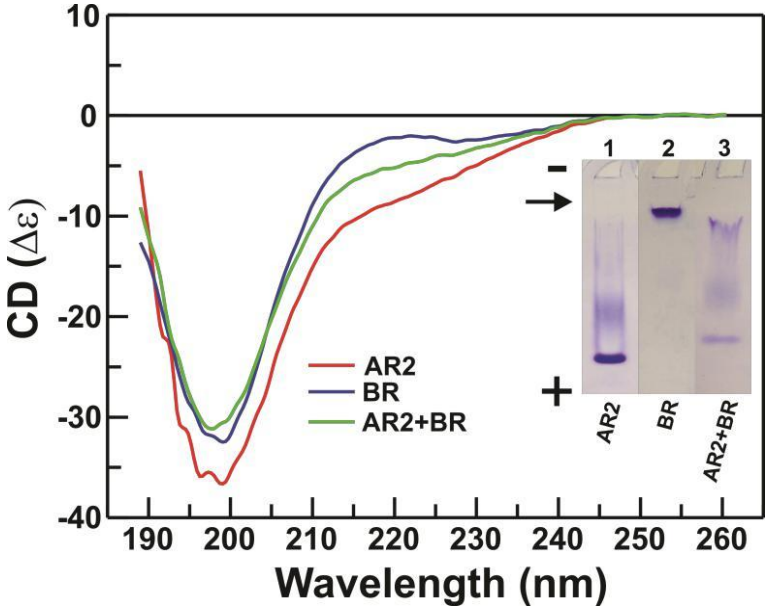

Figure 2. **CD spectra of FV-AR2 peptide, FV-BR peptide and equimolar mixture of each.** The observed far UV CD spectra of FV-AR2 (red), FV-BR (blue) and of FV-AR2+FV-BR mixture (green) in 20 mM sodium phosphate at pH 8.0 are shown. Analysis of these spectra with CONTIN program indicated that these moieties contain ~20% helical content and no β-sheet. Inset, Native PAGE gels (15% acrylamide) of FV-AR2 (lane 1), FV-BR (lane 2) and FV-AR2+FV-BR equimolar mixture (lane3).

Top five modeled structures of each peptide (FV-AR2 and FV-BR) were retrieved from the ITASSER server.[15] One structure for each FV-AR2 (Figure 3A) and FV-BR (Figure 3B) was selected for docking experiments based upon their QMEAN[16] and ModFOLD[17] scores as well as the secondary structural contents obtained from the CD data. The

QMEAN score for FV-AR2 was 0.69 and for FV-BR was 0.49, indicating a high probability for each structure in its native state. Additionally, the ModFOLD server revealed high confidence level for each structure with a *p*-value of $3.72E^{-3}$ for FV-AR2, and $2.78E^{-3}$ for FV-BR; these parameters further validate the reliability of the proposed structures. Importantly, in both FV-AR2 and FV-BR, the hydrophobic residues are packed inside the core of each molecule (Figures 3A and 3B), whereas the charged residues are exposed to the surface for the proposed electrostatic interactions.

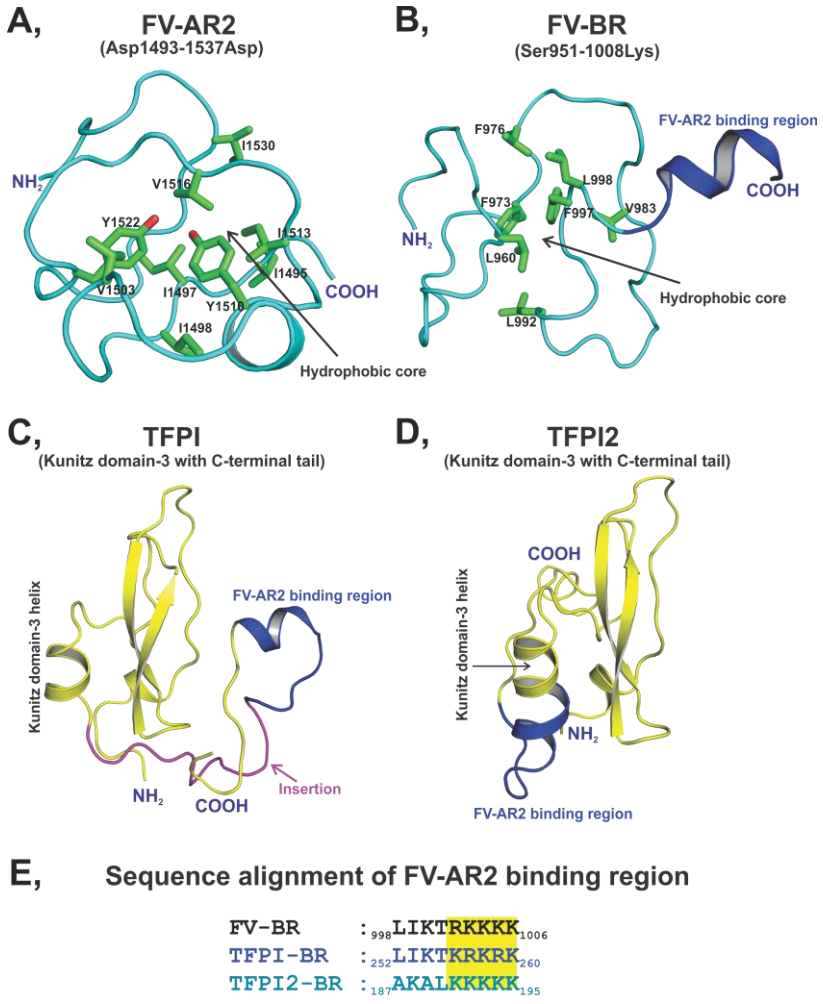

Figure 3. **Modeled structures of FV-AR2, FV-BR and the Kunitz domain-3 of TFPI and TFPI2 with their C-terminal basic regions.** ***A***, Cartoon representation of the modeled FV-AR2 segment from Asp1493 to Asp1537. The hydrophobic residues in the core region are shown in stick representation. Carbon atoms are green and oxygen atoms are red. Note that Tyr1510 and Tyr1522 are part of the hydrophobic core but their hydroxyl groups are exposed to the surface and participate in ligand interactions. **B**, Cartoon representation of the modeled FV-BR segment from Ser951 to Lys1008. As above, the hydrophobic residues in the core region are shown in stick representation. **C,** Cartoon representation of the Kunitz domain-3 of TFPI with its C-terminal tail. The region linking the C-terminal end of the Kunitz domain and the conserved FV-AR2 binding region is shown in magenta. The conserved FV-AR2 binding region is in blue. **D**, Cartoon representation of the Kunitz domain-3 of TFPI2 with its C-terminal tail. Note that the conserved FV-AR2 binding region is part of the C-terminal helix and is shown in blue. **E**, Amino acid sequences of the conserved nine-residue segments of FV-BR, TFPI-BR and TFPI2-BR. The five basic residues continuous in each sequence are shaded in yellow.

Similar to FV-AR2 and FV-BR, quality assessment results from the ModFOLD server gave high confidence levels and *p*-values for the modeled structures of the Kunitz domain-3 of TFPI ($2.6E^{-3}$) and TFPI2 ($9.4E^{-4}$) with their C-terminal basic regions (Figure 3C and 3D). Notably, in the modeled structures of FV-BR, TFPI and TFPI2, the conserved nine residue segments (Figure 3E) which are implicated in binding to the FV-AR2 region adopt similar conformations (Figures 3B, 3C and 3D).

The interactions of FV-AR2 with FV-BR, TFPI-BR and TFPI2-BR are shown in Figure 4. The FV-AR2 region has a well-defined acidic groove and electrostatic shape complementary to accommodate the five continuous basic amino acids in the homologous nine-residue peptide sequence shown in Figure 3E. The residues involved in making the acidic groove in FV-AR2 are labeled in black in Figures 4A, 4B and 4C. In the modeled complexes, part of the conserved region in FV-BR, TFPI-BR and TFPI2-BR adopt helical conformation. Since the homologous segment in FV-BR, TFPI-BR and TFPI2-BR adopt similar conformations, all of them fit well into the charge and shape complementary binding pocket of FV-AR2 region (Figure 4). All five continues Arg/Lys residues in FV-BR, TFPI-BR and TFPI2-BR are involved in the complex formation. The shape complementarity score for the complexes of FV-AR2:FV-BR, FV-AR2:TFPI-BR and FV-AR2-TFPI2-BR are 0.68, 0.71 and 0.68, respectively, indicating excellent fit for each. The residues that form hydrogen bonds and salt bridges between the FV-AR2 and its binding partners are listed in Table 1. In each case, comparable electrostatic interactions play a central role in forming the bimolecular complexes.

In previous studies, surface plasmon resonance data (SPR) yielded K_d values of 48 nM and 36 nM for binding of FV-1033 to TFPI and TFPI2, respectively.[4] Note that FV-1033 is recombinant FV in which B-domain residues 1034-1491 have been deleted; however, it contains both FV-BR and FV-AR2 regions and is equivalent to full-length FV in all biological properties.[24] Moreover, the affinity of TFPI binding to full-length FV has been reported to be ~15 nM,[25] a value close to 36 nM for FV-1033.[4] Noticeably, steady-state fluorescence anisotropy studies yielded a K_d value of 0.09 nM for binding of FV-810 (lacking the BR region) to TFPI.[3] Almost ~370-fold reduced affinity for binding of TFPI (and presumably TFPI2) to full-length FV and FV-1033 implies that FV-AR2 must first dissociate from the internal FV-BR region to permit binding of TFPI (or TFPI2). Since the binding of FV-AR2 to the internal FV-BR region is primarily electrostatic in nature (Figure 4A), it implies rapid association and dissociation rates for this interaction that promote binding of transient free FV-AR2 to TFPI or TFPI2. Under the SPR experimental conditions, such a mechanism could shift the equilibrium and generate additional free FV-AR2 for binding to TFPI or TFPI2.[4] Moreover, as compared to TFPI, TFPI-BR (K_d ~0.43 nM) or FV-BR peptide (K_d ~2 nM) has reduced affinity for FV-810[3,7]; this suggests that some additional interactions exist between TFPI (or TFPI2) and FV. A separate region (FV-AR1) involving acidic residues 659-DDDEDS-664 and/or 688-EDEESDADYD-697 in FV might be involved in such interactions.[4] Region(s) in TFPI or TFPI2 that could interact with these additional acidic residues in FV is not known.

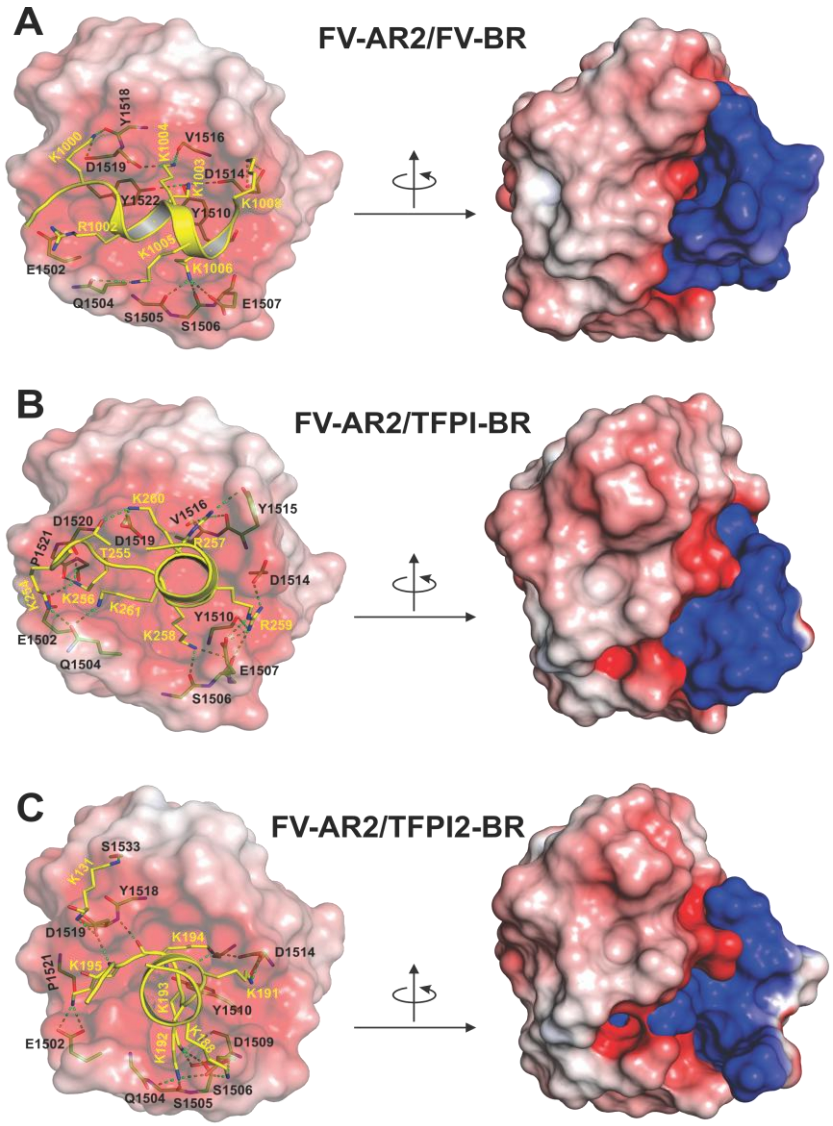

Figure 4. **Molecular interactions between the modeled complexes of FV-AR2 peptide with FV-BR peptide, TFPI-BR or TFPI2-BR.** ***A***, The molecular interactions between the FV-AR2 and FV-BR regions. The electrostatic surface of the FV-AR2 peptide and a cartoon representation of the FV-BR peptide (yellow) are depicted. ***B***, the molecular interactions between FV-AR2 and the TFPI-BR. As in ′***A***′, the electrostatic surface of the FV-AR2 peptide and a cartoon representation of the TFPI-BR (yellow) are depicted. ***C***, the molecular interactions between FV-AR2 and the TFPI2-BR. As in ′***A***′ and ′***B***′, the electrostatic surface of the FV-AR2 peptide and a cartoon representation of the TFPI2-BR (yellow) are depicted. The residues that form hydrogen bonds and salt bridges in ***A***, ***B*** and ***C*** are shown in stick representation. For each complex, the electrostatic surface of the interacting molecular species is shown on the right; this view represents a 90° rotation along the vertical axis. The electrostatic potential surfaces were calculated using the program APBS[23] and are drawn at ± 5 kT/e. Carbon, oxygen and nitrogen atoms are in yellow, red and blue, respectively. The hydrogen bonds are shown in cyan dashed lines. The blue represents positive charge, red represents negative charge, and white represents neutral charge.

Table 1. Salt bridge and H-bond interactions of FV-AR2 with FV-BR, TFPI-BR and TFPI2-BR

FV-AR2 Residues	FV-BR Residues	TFPI-BR Residues	TFPI2-BR Residues	Type of Interaction
Glu1496 (mc C=O)			Lys194	H-bond
Glu1502	Arg1002	Lys254, Lys256	Lys195	Salt-bridge
Gln1504 (mc C=O)			Lys192	H-bond
Gln1504	Lys1005	Lys254, Lys258		H-bond
Ser1505 (mc C=O)	Lys1006		Lys192, Lys193	H-bond
Ser1506 (mc C=O)	Lys1006	Lys258		H-bond
Glu1507 (mc C=O)		Lys258, Arg259		H-bond
Glu1507	Lys1006	Lys258, Arg259		Salt-bridge
Asp1509			Lys193	Salt-bridge
Tyr1510 (mc C=O)		Arg259		H-bond
Tyr1510	Lys1003	Arg259	Lys194	H-bond
Ile1513 (mc C=O)			Lys194	H-bond
Asp1514(mc C=O)	Lys1003			H-bond
Asp1514	Lys1008		Lys191	Salt-bridge
Tyr1515 (mc C=O)		Arg257		H-bond
Tyr1515		Arg257		H-bond
Val1516 (mc C=O)	Lys1004	Arg257		H-bond
Pro1517 (mc C=O)				H-bond
Tyr1518 (mc C=O)	Lys1000		Lys194 (mc)	H-bond
Asp1519 (mc C=O)	Lys1000	Lys260	Met196 (mc)	H-bond
Asp1519	Lys1004		Lys131 (mc)	H-bond
Asp1520 (mc C=O)		Lys256		H-bond
Pro1521		Lys256	Lys195	H-bond
Tyr1522	Lys1003			H-bond
Ser1533 (mc C=O)			Lys131	H-bond

mc, main chain

In additional studies, Western blot analysis revealed binding of FVa (lacking both the BR and the AR2 regions) to TFPI.[26] In SPR experiments, the affinity of FVa binding to TFPI was ~460 nM and to TFPI2 ~250 nM.[4] In ELISA experiments, the affinity of FVa binding to TFPI2 was ~100 nM.[4] The interaction of TFPI or TFPI2 with FVa that lacks the FV-AR2 region could involve FV-AR1 region (659-DDDEDS-664 and/or 688-EDEESDADYD-697 residues). These observations indicate that in addition to the FV-AR2 region, other regions (e.g., FV-AR1) in FV might provide specificity for interaction with the basic region segments in FV, TFPI and TFPI2.

4. Conclusion

In conclusion, we have directed our efforts in this report towards identifying the key residues involved in the interaction between FV-BR, TFPI or TFPI2 with FV-AR2. We combined the available experimental data with the structures obtained from the protein modeling/docking servers that are top ranked in the recent critical assessment of the protein structure prediction/docking

algorithms. Our each selected modeled structure possesses the characteristic nature of a folded protein in which the polar residues are exposed to the surface, while the non-polar residues are buried inside the core of the molecule. The evaluation of the predicted structures using different methods substantiate the proposed modeled interactions. Of significance is the observation that the modeled structure of FV-AR2 has a compact fold with a complementary charged groove to optimally accommodate the conserved basic residues of FV-BR, TFPI-BR or TFPI2-BR. Experimentally determined structures using crystallography and/or NMR are needed to validate the proposed interactions. In the interim, these models provide a framework for appropriate mutagenesis experiments to further understand the molecular and biological significance of TFPI or TFPI2 interaction with FV/FVa.

ACKNOWLEDGEMENTS

This work was supported by National Heart, Lung and Blood Institute grant 5R21HL122878 (SPB), R01HL88010 (RMC) and P01HL74124 (RMC).

The authors declare that they have no competing financial interest.

REFERENCES

[1]. Broze GJ Jr, Girard TJ. Tissue factor pathway inhibitor: structure-function. *Front Biosci*, 2012; **17**: 262–80.

[2]. Chand HS, Foster DC, Kisiel W. Structure, function and biology of tissue factor pathway inhibitor-2. *Thromb Haemost*, 2005; 94(6):1122–30.

[3]. Wood JP, Bunce MW, Maroney SA, Tracy PB, Camire RM, Mast AE. Tissue factor pathway inhibitor-alpha inhibits prothrombinase during the initiation of blood coagulation. *Proc Natl Acad Sci USA* 2013; 110(44): 17838-43.

[4]. Vadivel K, Ponnuraj SM, Kumar Y, Zaiss AK, Bunce MW, Camire RM, Wu L, Evseenko D, Herschman HR, Bajaj MS, Bajaj SP. Platelets contain tissue factor pathway inhibitor-2 derived from megakaryocytes and inhibits fibrinolysis. *J Biol Chem* 2014; 289(45): 31647-61.

[5]. Jenny RJ, Pittman DD, Toole JJ, Kriz RW, Aldape RA, Hewick RM, Kaufman RJ, Mann KG. Complete cDNA and derived amino acid sequence of human factor V. *Proc Natl Acad Sci USA* 1987; 84(14): 4846-50.

[6]. Bos MH, Camire RM. A bipartite autoinhibitory region within the B-domain suppresses function in factor V. *J Biol Chem* 2012; 287(31): 26342-51.

[7]. Bunce MW, Bos MH, Krishnaswamy S, Camire RM. Restoring the procofactor state of factor Va-like variants by complementation with B-domain peptides. *J Biol Chem* 2013; 288(42): 30151-60.

[8]. Monkovic DD, Tracy PB. Activation of human factor V by factor Xa and thrombin. *Biochemistry* 1990; 29(5): 1118–28.

[9]. Thorelli E, Kaufman RJ, Dahlback B. Cleavage requirements for activation of factor V by factor Xa. *Eur J Biochem* 1997; 247(1): 12–20.

[10]. Monkovic DD, Tracy PB. Functional characterization of human platelet-released factor V and its activation by factor Xa and thrombin. *J Biol Chem* 1990; 265(28):17132–40.

[11]. Vincent LM, Tran S, Livaja R, Bensend TA, Milewicz DM, Dahlbäck B. Coagulation factor V(A2440G) causes east Texas bleeding disorder via TFPIα. *J Clin Invest* 2013; 123(9): 3777-87.

[12]. Cunha ML, Bakhtiari K, Peter J, Marquart JA, Meijers JC, Middeldorp S. A novel mutation in the F5 gene (factor V Amsterdam) associated with bleeding independent of factor V procoagulant function. *Blood* 2015; 125(11): 1822-25.

[13]. Whitmore L, Wallace BA. DICHROWEB, an online server for protein secondary structure analyses from circular dichroism spectroscopic data. *Nucleic Acid Res.* 2004; 32(Web Server issue):W668-673.

[14]. Whitmore L, Wallace BA. Protein secondary structure analyses from circular dichroism spectroscopy: methods and reference databases. *Biopolymers* 2008; 89(5): 392-400.

[15]. Zhang Y. I-TASSER server for protein 3D structure prediction. BMC *Bioinformatics* 2008; 9: 40.

[16]. Benkert P, Tosatto SCE, Schomburg D. QMEAN: A comprehensive scoring function for model quality assessment. *Proteins Struct Funct Bioinf* 2008; 71(1): 261-77.

[17]. McGuffin LJ, Buenavista MT, Roche DB. The ModFOLD4 Server for the Quality Assessment of 3D Protein Models. *Nucleic Acids Res* 2013; 41(Web Server issue): W368-72.

[18]. Berman HM, Westbrook J, Feng Z, Gilliland G, Bhat TN, Weissig H, Shindyalov IN, Bourne PE. The Protein Data Bank. *Nucleic Acids Res* 2000; 28(1): 235-42.

[19]. Mine S, Yamazaki T, Miyata T, Hara S, Kato H. Structural mechanism for heparin-binding of the third Kunitz domain of human

tissue factor pathway inhibitor. Biochemistry 2002; 41(1):78-85.

[20]. Macedo-Ribeiro S, Almeida C, Calisto BM, Friedrich T, Mentele R, Stürzebecher J, Fuentes-Prior P, Pereira PJ. Isolation, cloning and structural characterisation of boophilin, a multifunctional Kunitz-type proteinase inhibitor from the cattle tick. PLoS One 2008; 3(2):e1624.

[21]. Brooks BR, Brooks CL 3rd, Mackerell AD Jr, Nilsson L, Petrella RJ, Roux B, Won Y, Archontis G, Bartels C, Boresch S, Caflisch A, Caves L, Cui Q, Dinner AR, Feig M, Fischer S, Gao J, Hodoscek M, Im W, Kuczera K et al. CHARMM: the biomolecular simulation program. *J Comput Chem* 2009; 30(10): 1545-614.

[22]. Comeau SR, Gatchell DW, Vajda S, Camacho CJ. ClusPro: a fully automated algorithm for protein-protein docking. *Nucleic Acids Res* 2004; 32(Web Server issue): W96-W99.

[23]. Baker NA, Sept D, Joseph S, Holst MJ, McCammon JA. Electrostatics of nanosystems: application to microtubules and the ribosome. *Proc Natl Acad Sci USA* 2001; 98(18): 10037-41.

[24]. Zhu H, Toso R, Camire RM. Inhibitory sequences within the B-domain stabilize circulating factor V in an inactive state. J Biol Chem 2007;282(20):15033-9.

[25]. Duckers C, Simioni P, Spiezia L, Radu C, Gavasso S, Rosing J, Castoldi E. Low plasma levels of tissue factor pathway inhibitor in patients with congenital factor V deficiency. *Blood* 2008; 112(9): 3615–23.

[26]. Ndonwi M, Girard TJ, Broze GJ Jr. The C-terminus of tissue factor pathway inhibitor α is required for its interaction with factors V and Va. *J Thromb Haemost* 2012; 10(9): 1944–46.

